



SO/PHI
POLARIMETRIC AND HELIOSEISMIC IMAGER
FOR SOLAR ORBITER

ISPFI CF-252 TEST RESULTS

reference	SOL-PHI-MPS-TD3000-RP-5
issue	1(prel)
revision	0
release date	2012-04-24
prepared by	J. Piqueras, S. Werner
approved by	K. Heerlein



ISPFI CF-252 TEST RESULTS

ADDITIONAL DISTRIBUTION

NAME	ORGANISATION
PHI Document Database	
K. Heerlein, S. Werner, U. Schühle, J. Woch , R. Enge, J. Piqueras	MPS

CHANGE LOG

REASON FOR CHANGE	ISSUE	REVISION	DATE
Initial issue	1	0	2012-04-24

CHANGE RECORD

changes published in issue: 1(prel) revision: 0

REASON FOR CHANGE	SECTION(S)	PAGE(S)



ISPHI CF-252 TEST RESULTS

TABLE OF CONTENTS

1. INTRODUCTION.....5

2. TEST DESCRIPTION5

3. RESULTS OF LIVE TEST7

4. RESULTS OF PRE/POST- TEST CHARACTERIZATION11

4.1. DARK CURRENT 12

4.2. DARK CURRENT NON-UNIFORMITY12

4.3. SIGNAL AND SATURATION LEVELS 13

4.4. PIXEL RESPONSE NON-UNIFORMITY 14

4.5. BAD PIXELS 14

5. SUMMARY AND CONCLUSIONS15

DOCUMENT REFERENCES.....16

5.1. NORMATIVE REFERENCES 16

5.2. INFORMATIVE REFERENCES 16

6. ACRONYMS17



ISPHI CF-252 TEST RESULTS

LIST OF FIGURES

Figure 2-1 Vacuum jail with camera inside (left) and camera electronics with sensor and Cf-252 source (right).. 5

Figure 2-2 Experimental set-up while test is running..... 6

Figure 3-1 Dark image (sub-area) during irradiation: Beginning (left) and end (right) of test. White dots appear across the whole array, and at the end of the test, the induced non-uniformity forms a background fixed pattern noise. 8

Figure 3-2 Current consumption HK versus irradiation run. The x-axis' run numbers define the start of that irradiation period. 8

Figure 3-3 TMR error vector recovered via HK. The x-axis run numbers defines the start of that irradiation period. 9

Figure 3-4 Camera main supplies during irradiation. 9

Figure 3-5 Pixels supplies during irradiation. 9

Figure 3-6 Monitoring of the mean value of the acquired dark frames during irradiation. The mean value is calculated separately for the four areas that correspond to different output stages of the sensor. The identified SEEs are marked, as well as two events (**) that respond to external reasons (illumination changes). 10

Figure 3-7 Monitoring of the spatial standard deviation of the acquired dark frames during irradiation. The std value is calculated separately for the four areas that correspond to different output stages. 10

Figure 3-8 Monitoring of the number of hot pixels during irradiation. The used criterion is that a pixel is hot if its value is, at least, six times higher than the standard deviation. 11

Figure 4-1 Dark current: Measurements before and after irradiation/annealing. 12

Figure 4-2 Dark current non-uniformity at 100 ms of exposure time: Measurements before and after irradiation/annealing. 13

Figure 4-3 Mean flat level before and after irradiation/annealing. 13

Figure 4-4 Pixel response non-uniformity: Measurements before and after irradiation/annealing..... 14

Figure 4-5 Bad pixels on the flat images at 100 ms of exposure time. The measurement criterion is above or below 6 times the standard deviation. 14

LIST OF TABLES

Table 2-1 Test conditions 6

Table 2-2 Summary of irradiation runs. 6

Table 2-3 Summary of pre and post characterization test 7

Table 2-4 Measurements performed before and after irradiation/annealing. 7

Table 3-1 List of identified SEEs. 11

Table 5-1 Summary of Cf-252 effects 15

1. INTRODUCTION

This document reports on the results of the Californium-252 radiation test performed with the ISPHI. This test was carried out as a pre-heavy ions test to assess the behavior of the sensor under low fluence HI irradiation, and to check the suitability of the PHI camera electronics (Breadboard model) as a control/monitoring system during irradiation. Therefore, this test does not replace the heavy ions one included in the radiation test plan [IR01], but serves as a preparation for that experiment.

2. TEST DESCRIPTION

The Cf-252 heavy ions campaign was carried out at ESTEC, using a CASE system [IR12], from 2 to 3 April 2012. After the irradiation and continuous monitoring of images to detect single event effects, the devices were annealed at room and high temperature to study long-term effects that the irradiation may have provoked. The annealing phase extended until 19 April 2012.

The heavy ions irradiation mainly focuses on the study of single event effects on electronic devices. However, it may also lead to long-term degradation of some sensor parameters due to ionizing effects. Consequently, two kinds of measurements were performed during the campaign: The live measurements during irradiation to test for SEE, and the pre and post irradiation and annealing characterization to evaluate the long-term degradation. Only one device (10021) was tested.

The irradiation setup is shown in Figure 2-1 and Figure 2-2. On the first picture, the camera electronics with the sensor on it is placed inside the vacuum jail where the test shall run. The right side includes a closer look where the source is already placed on its holder and the image sensor is visible. The test cable, specifically built for this experiment, is also connected to the jail feed-through. The source holder can be moved to hit specific parts of the sensor, or to place it apart. Note that the irradiated area is smaller than the physical size of the detector. Therefore, the source shall be moved during the test to get guarantee that every part of the detector receives particle radiation.

The second figure displays an overview of the test while running, where the control computer, the power supply and EGSE can be seen. The vacuum jail is covered during the test to block the light and get dark images on the detector. On the right side, the vacuum meter measures the pressure level inside the jail, which is created by an external vacuum pump.

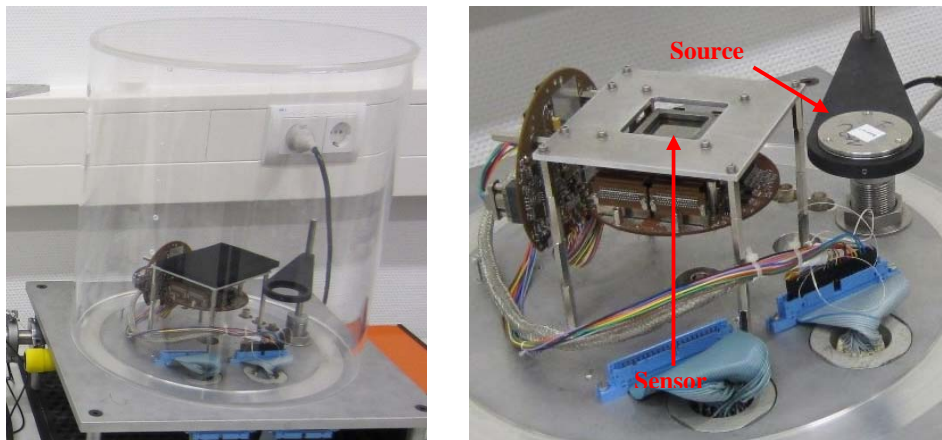


Figure 2-1 Vacuum jail with camera inside (left) and camera electronics with sensor and Cf-252 source (right).

ISPFI CF-252 TEST RESULTS

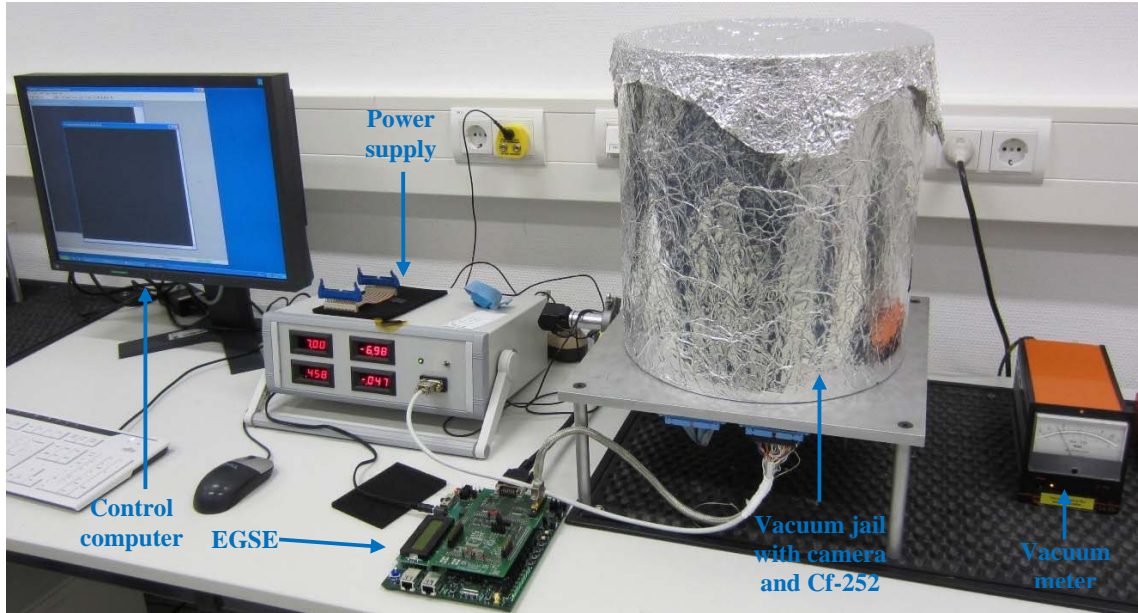


Figure 2-2 Experimental set-up while test is running.

The test conditions are summarized in Table 2-1, whereas the set of irradiation runs are in Table 2-2. This table indicates the periods on which the sensor ran continuously¹ with the source on its top. The source location refers to the sensor area that was hit by the irradiated particles. The number of images per cycle indicates the frequency of housekeeping acquisition. A value of n means that a set of HKs is taken every n frames. Note that the first version of the Ruediger software was employed, and only single acquisitions were allowed. Finally, the TMR functionality was introduced on the BBM for this test. If TMR is enable, the camera electronics checks the status of the sensor SPI registers after every acquisition, keeps a record of found errors, and re-writes the correct value in case of failure. In this way, the camera provides the sensor with a remote TMR against single event upsets (SEU) on the sensor registers.

Source	Cf-252	
LET (MeV cm ² /mg)	43	Average level
Flux (ions/cm ² /min)	3000	The exact flux was not measured, but it is estimated between 2500 and 3500
Range [Si] (µm)	< 15	Value taken from [IR13]
Temperature (degC)	Room	Not controlled but monitored RT
Vacuum (bar)	6 10 ⁻²	TBC
IS cover	No glass	Cover glass was removed
Exposure time (ms)	50	Dark exposures
Readout freq. (MHz)	30	Maximum frequency

Table 2-1 Test conditions

	Time	Source location	Images/cycle	TMR
Run 1	08:43 – 09:45	Center	10	ON
Run 2	09:55 – 10:55	Edge (gold stripe)	10	ON
Run 3	11:01 – 12:08	Edge (opposite to gold)	1	ON
Run 4	12:12 – 13:12	Center	10	OFF
Run 5	13:19 – 14:19	Edge (gold stripe)	10	OFF
Run 6	14:21 – 15:21	Edge (opposite to gold)	10	OFF
Run 7	15:23 – 17:40	Center	1	ON
Run 8	17:44 – 18:08	Center	1	ON

Table 2-2 Summary of irradiation runs.

¹ The acquisition was continuous but there was a duty cycle lower than 100% because of HK acquisition and image storage. This duty cycle is lower for 1 image/cycle than for 10 images/cycle.

All images acquired during the test were saved in the control computer, so that a post-analysis of the potential SETs and SEFIs is possible. This version of the camera electronics (BBM) did not include a dedicated latch-up protection for the sensor, though the power supply had a limitation of 1.5A for the main supply. At the same time, a HK was continuously monitored and saved for the total current consumption. However, the updating rate of this HK was not enough as to monitor any SEL.

As for the measurements made to determine the long-term changes on the sensor parameters, the same set was carried out before irradiation, after irradiation, and at every annealing step (Table 2-3). Table 2-4 gives a summary of the set of measurements, which consists on target images using different sensor output configurations, dark images versus exposure time, and flat images versus exposure time. The evaluation board was used for this characterization.

The employed optical testbench consists of a halogen white source, a green filter ($\lambda=550\text{nm}$; $\Delta\lambda_{\text{FWHM}}=10\text{nm}$), a set of lenses to reach the optimum focus, the target and the camera. The evaluation board of CMOSIS, running at full speed (30 MHz) with the default gain and bias settings (see datasheet [IR04]), was used during the whole campaign. The temperature of the sensor could not be controlled during the measurements, especially during those made in the irradiation facility, but not extreme variations happened from measurement from measurement.

Device	Measurement	Fluence* [ions/cm ²]	Annealing
10021	Before test	0	-
	After test	1.5 10 ⁶	24 hr @ RT
	After ann. RT	1.5 10 ⁶	168 hr @ 21 °C
	After ann. HT	1.5 10 ⁶	168 hr @ 21 °C + 168 hr @ 100 °C

Table 2-3 Summary of pre and post characterization test

Measurement	ISPHI mode	Exposure times (ms)	# images / point
Target	1CH-HV 1CH-LV 2CH-HV 2CH-LV	100	3
Dark	2CH-HV	0, 1, 5, 10, 30, 50, 70, 100, 200, 500, 1000, 5000	10
Flat	2CH-HV	0, 1, 5, 10, 30, 50, 70, 100, 120, 140, 160, 180, 200, 220, 240, 260, 280, 300, 400, 500, 1000	10

Table 2-4 Measurements performed before and after irradiation/annealing.

3. RESULTS OF LIVE TEST

The aim of the live test is the identification of single event effects that may alter the normal functionality of the sensor. This section reviews the housekeeping values, image appearance and some image statistics over the sequences of images taken at every irradiation run. At the end of the section a summary of the identified events along with their evidences is given.

The first noticeable effect after placing the radioactive source over the sensor was that random white dots appeared across the whole array. These spurious pixels vary from image to image, and are related to the generation of electron-holes induced by the irradiated particles. On the left side of Figure 3-1, a set of white dots can be distinguished over the dark background. After the sensor had been exposed to radiation for a while, the white spots continue appearing but a fixed pattern noise emerges on the background of the dark images. This gradual increase in fixed pattern noise is a long-term effect, thus it will be analyzed in Section 4. In general, the temporal white pixels on the image are a regular consequence of the semiconductor nature of the sensor, and not a damage provoked by radiation.

One of the regularly acquired HK is the total current consumption, which is displayed in Figure 3-2 for complete campaign (eight runs). This current corresponds to the 5V main supply, meaning that on average the consumption is of about 2.6W. The high frequency fluctuations of the measured current are due to the fact that

ISPFI CF-252 TEST RESULTS

the housekeeping acquisitions are synchronized by the software, therefore not all were acquired during the same state of the acquisition (for instance, the consumption is higher in the middle of one image than in the transition between frames). In any case, it can be clearly seen that during run 4 the consumption suffered a sudden rise that does not disappear until the run is finished and the camera is power cycled. The increase is about 200mW. As we will see after analyzing the image statistics, this event corresponds to a SEE.

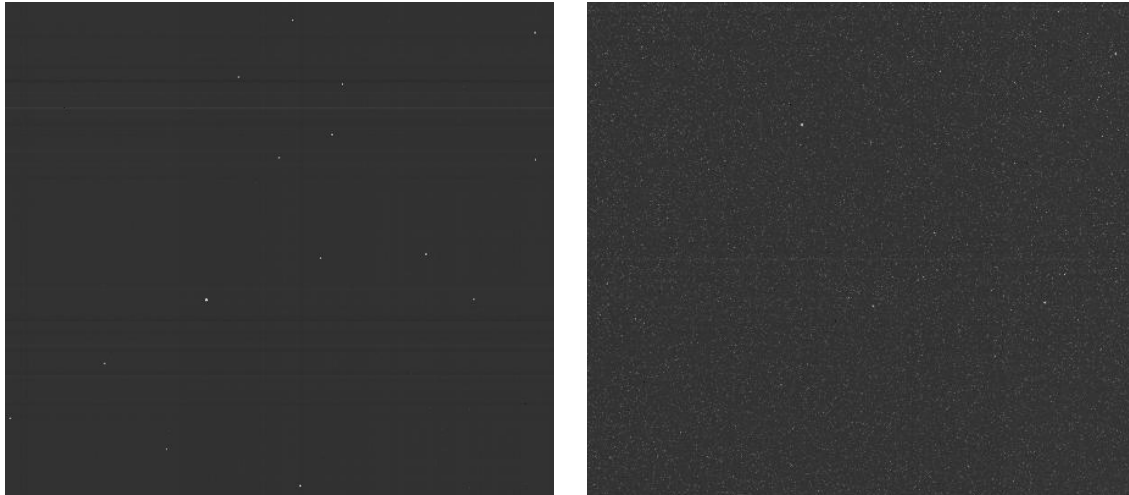


Figure 3-1 Dark image (sub-area) during irradiation: Beginning (left) and end (right) of test. White dots appear across the whole array, and at the end of the test, the induced non-uniformity forms a background fixed pattern noise.

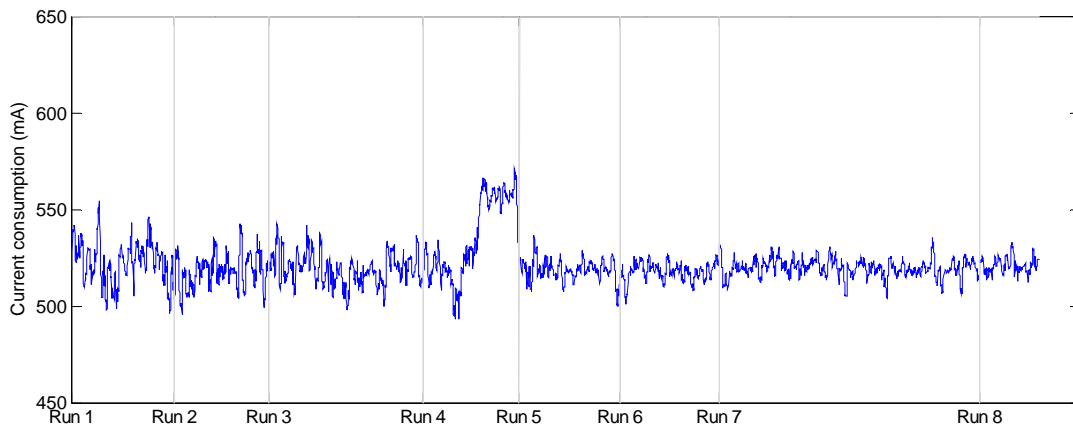


Figure 3-2 Current consumption HK versus irradiation run. The x-axis' run numbers define the start of that irradiation period.

As it was explained in Section 2, the remote TMR functionality allows the detection and correction of SEUs on the SPI register of the sensor when this option is enable. During runs 4, 5 and 6 it was disable, and during runs 1 and 2 it was enable but HKs were only acquired every 10 frames. This means that the SEU correction was working but it is possible that the HK containing the error vector of that correction was not acquired. From Figure 3-3, we can see that only one SEU was reported via the TMR error detection at the beginning of run 8. This event corresponds to the register number 32, which is the CMREFLV (reference level of the sensor output). The later analysis of the image statistics, together with the known effect of changing this register value, will confirm the existence of such an event.

ISPHI CF-252 TEST RESULTS

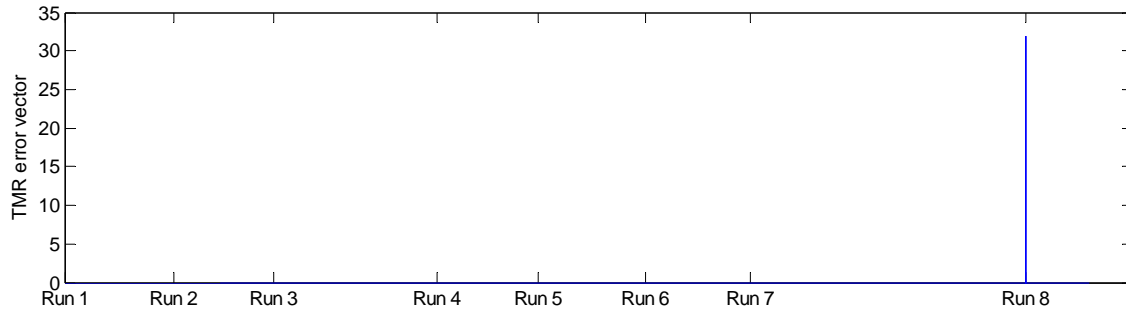


Figure 3-3 TMR error vector recovered via HK. The x-axis run numbers defines the start of that irradiation period.

The main and pixel supplies' housekeepings are shown in Figure 3-4 and Figure 3-5, respectively. It can be observed that no abnormal variations can be identified on those voltage levels.

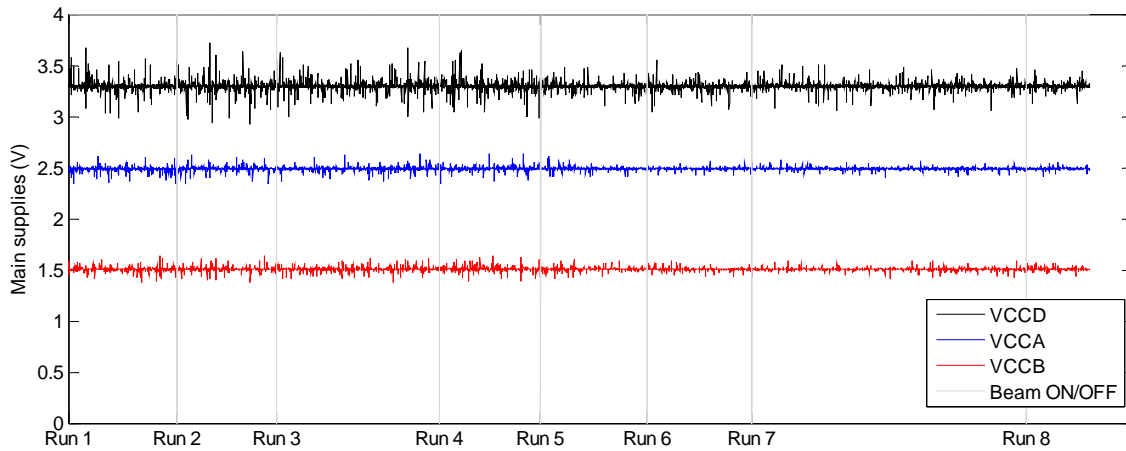


Figure 3-4 Camera main supplies during irradiation.

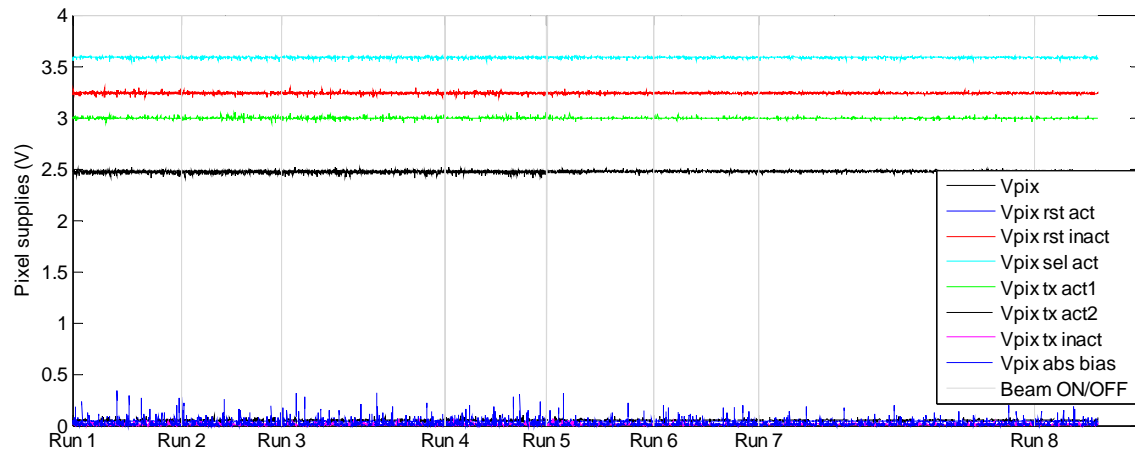


Figure 3-5 Pixels supplies during irradiation.

Most of the SEEs will be extracted from Figure 3-6. This graph shows the image mean value during the sequence of irradiations for every area of the image sensor. Every sudden change or peak is susceptible of being a single event effect. The only exceptions are during the test images taken after one run finishes and before the next one starts, and those mark with (**), which correspond to on purpose change on the darkness of the camera environment. The rest of highlighted events are sudden changes on the mean value, and are thus labeled as SEEs. Some of them are confirmed by the previous analyzed graphs, as for example the SEE5, which correspond to the

ISPFI CF-252 TEST RESULTS

increase in current consumption seen in Figure 3-2, and SEE7, which matches the TMR SEU reported on Figure 3-3. The actual values of the changes vary from 15 DN in SEE2 to more than 130 DN in SEE5. The visual analysis of the images ratifies that the variations on the mean value are over the complete array, and not due to some transient of pixels or bright area. This last remark suggests that they are probably related to SEUs.

Also important is to check that SEE1, SEE2 and SEE7 appear as a peak change that only affects a single frame, whereas SEE3, SEE4, SEE5 and SEE6 are a sudden change which effect continues until the run finishes and/or the camera is power cycled. This is because runs 2 and 8, where SEE1, SEE2 and SEE7 occur, have the TMR enable, and therefore the SEU is automatically corrected before the next image is acquired. However, the TMR is disabled for the rest of events where the effect is not recovered until the end of the run.

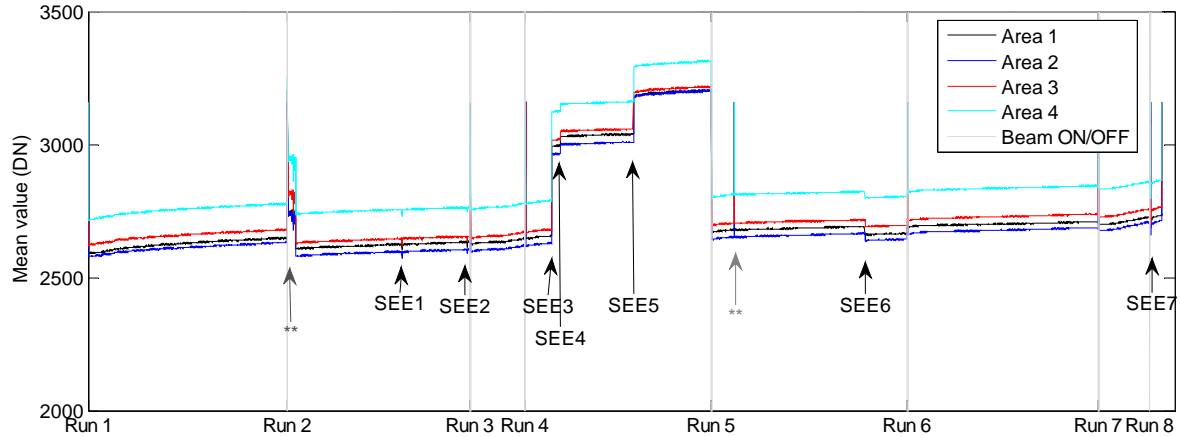


Figure 3-6 Monitoring of the mean value of the acquired dark frames during irradiation. The mean value is calculated separately for the four areas that correspond to different output stages of the sensor. The identified SEEs are marked, as well as two events (**) that respond to external reasons (illumination changes).

The same statistical analysis is done with the standard deviation of the four areas of the sensor. Some of the previously identified events (SEE2, SEE4, SEE6 and SEE7) appear also as a change on the std graph. As in the mean value examination, those events appearing with TMR enable recovers automatically whereas those without TMR only recovers at the end of the run.

Apart from the temporal events, a smooth increase on the image noise (or non-uniformity) is found from the beginning of the radiation test until the end. It is classified as a long-term effect and will be analyzed in Section 4.

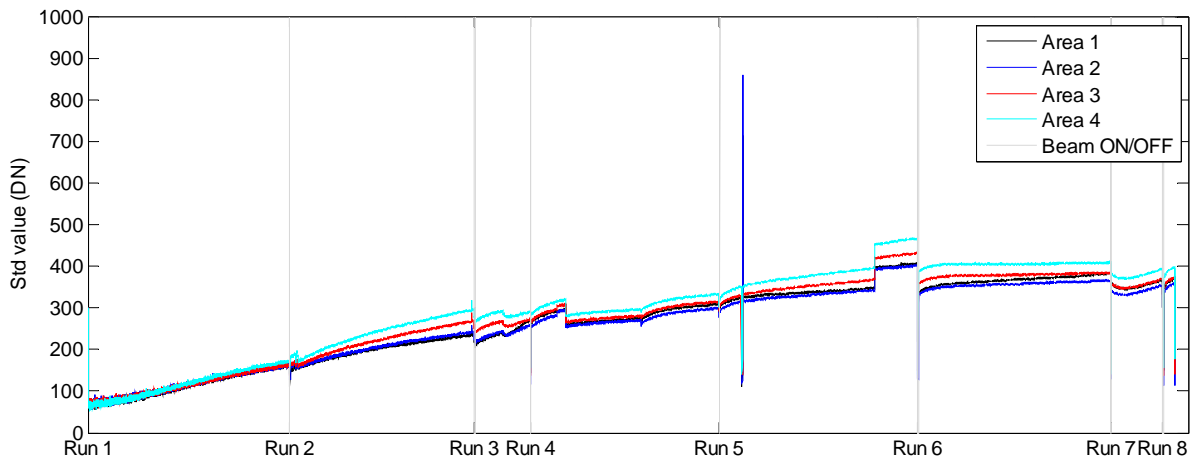


Figure 3-7 Monitoring of the spatial standard deviation of the acquired dark frames during irradiation. The std value is calculated separately for the four areas that correspond to different output stages.

Finally, the number of hot pixels on the images is analyzed during the irradiation sequence on Figure 3-8. Though this is more related to long-term effects, and the increase (except for the test images in the transitions and some known illumination changes) is smooth, the graph is included in this section because the live images have been used to generate it. The pre and post characterization also will deal with this analysis.



ISPFI CF-252 TEST RESULTS

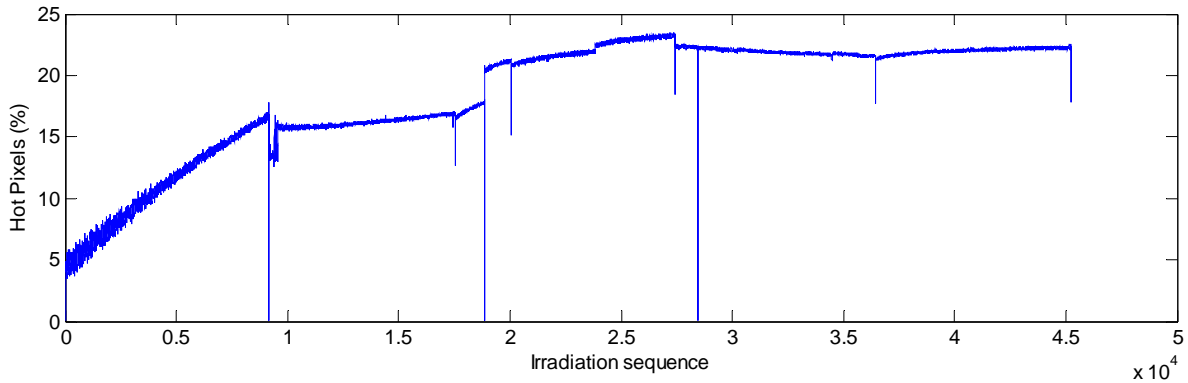


Figure 3-8 Monitoring of the number of hot pixels during irradiation. The used criterion is that a pixel is hot if its value is, at least, six times higher than the standard deviation.

Table 3-1 lists the seven recognized single event effects, summarizing on the last column the evidences that support their classification as SEEs. As for the location of the source above the sensor, events have been recorded with the source over the central part and the gold side part of the sensor, but no event was register on the opposite side. It may be because the registers are placed far from that area.

SEE	Run #	TMR Corrected	Time	Location on IS	Evidences
1(SEU)	2	Yes	10:33:08	Unknown	Mean value decreases about 30 DN during a single frame. TMR was ON but HK were only retrieved every 10 frames, so the error vector is missing.
2(SEU)	2	Yes	10:54:20	Unknown	Mean value decreases about 15 DN during a single frame. Standard deviation varies about 10 DN during a single frame. TMR was ON but HK were only retrieved every 10 frames, so the error vector is missing.
3	4	No (TMR OFF)	12:21:49	Unknown	Mean value suddenly increases about 330 DN and remains with that value. Standard deviation suddenly increases about 10 DN and remains with that value.
4	4	No (TMR OFF)	12:24:33	Unknown	Mean value suddenly increases about 25 DN and remains with that value. Standard deviation suddenly decreases about 40 DN and remains with that value.
5	4	No (TMR OFF)	12:48:08	Unknown	Mean value suddenly increases about 130 DN and remains with that value. Standard deviation suddenly decreases about 10 DN but slowly recovers. Power consumption suddenly increases about 200 mW, and this value is kept until power cycle.
6	5	No (TMR OFF)	14:06:23	Unknown	Mean value suddenly decreases about 25 DN, and remains with that value. Standard deviation suddenly increases about 55 DN, and remains with that value.
7(SEU)	8	Yes	17:44:56	Register 32	Mean value decreases about 50 DN for a single frame. TMR error vector is '1' for the register #32.

Table 3-1 List of identified SEEs.

4. RESULTS OF PRE/POST- TEST CHARACTERIZATION

The following subsections show how different parameters are affected after the irradiation campaign in contrast to the pre measurements. Some of the results will be given in absolute units (electrons). The gain factor used to convert from DN to e⁻, 0.029 DN/e⁻, is calculated and discussed in [IR07]. Therefore, in those cases where the units are electrons the DN could be obtained using the CG, and vice versa in those cases where the given values are in DN.

This section only presents the parameters that have shown any variation after irradiation, omitting those analyzed characteristics that remained unchanged.

4.1. DARK CURRENT

The measured dark current variation before, after irradiation and after annealing is shown in Figure 4-1. The level after irradiation is about 500 e⁻/s higher than the one measured before. Although this behavior is expected, the DC continues increasing during the first week of annealing at 21 degC until reaching a top level of more than 3500 e⁻/s. This last increase was not expected and the reason is not clear yet. After the annealing at 100 degC, the DC recovers a little bit, but it is still high compared to the initial value.

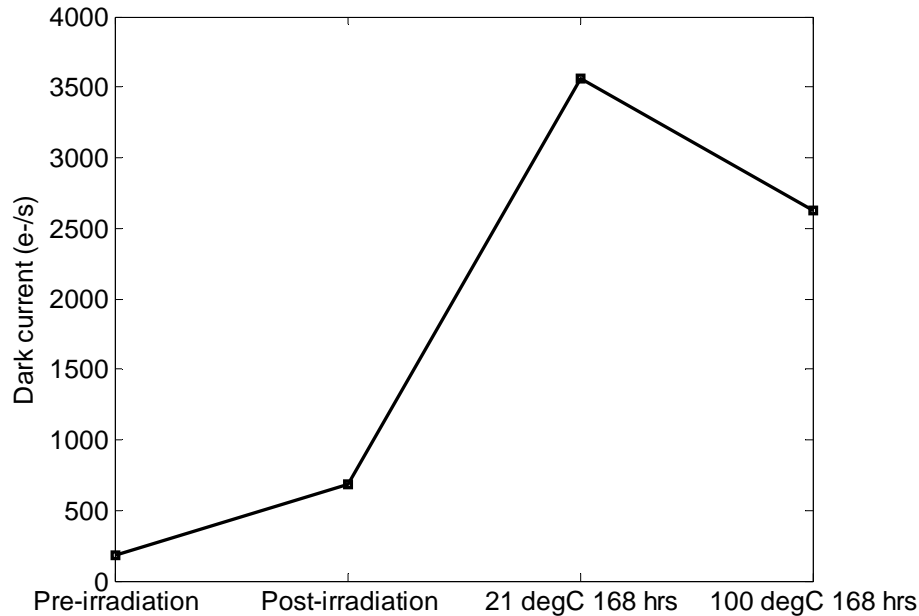


Figure 4-1 Dark current: Measurements before and after irradiation/annealing.

4.2. DARK CURRENT NON-UNIFORMITY

The non-uniformity on the dark current is displayed in Figure 4-2. It can be observed how after irradiation the value increases significantly, which agrees with the fixed pattern noise that was shown in Section 3 at the end of the test. After the first week of annealing at room temperature, the DCNU recovers a little bit, and after the annealing at high temperature the recovery is more pronounced. However, the initial value is not reached.

The DCNU has been measured as the standard deviation of a group of 800 x 800 pixels across a 10 frames averaged image. The bad pixels above 20 times the standard deviation were not included in this calculation.

ISPFI CF-252 TEST RESULTS

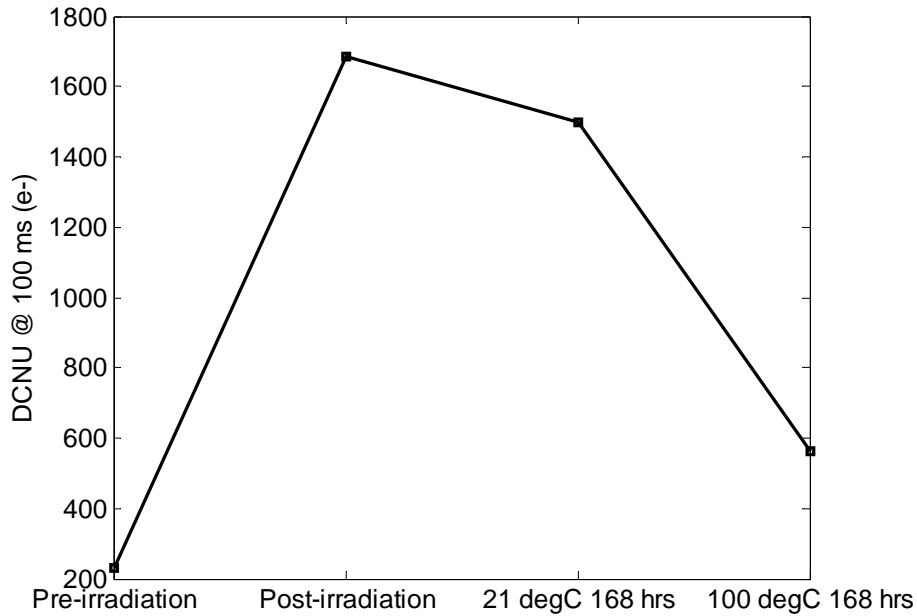


Figure 4-2 Dark current non-uniformity at 100 ms of exposure time: Measurements before and after irradiation/annealing.

4.3. SIGNAL AND SATURATION LEVELS

The level of the flat images is analyzed in Figure 4-3. Though there is a small variation on the response for the different measurements, it does not follow any pattern (for example, it is not better before irradiation). Therefore, it might be that the observe differences come from changes on the illumination or conditions (e.g. temperature) during measurements instead of real radiation effects. However, this is TBC.

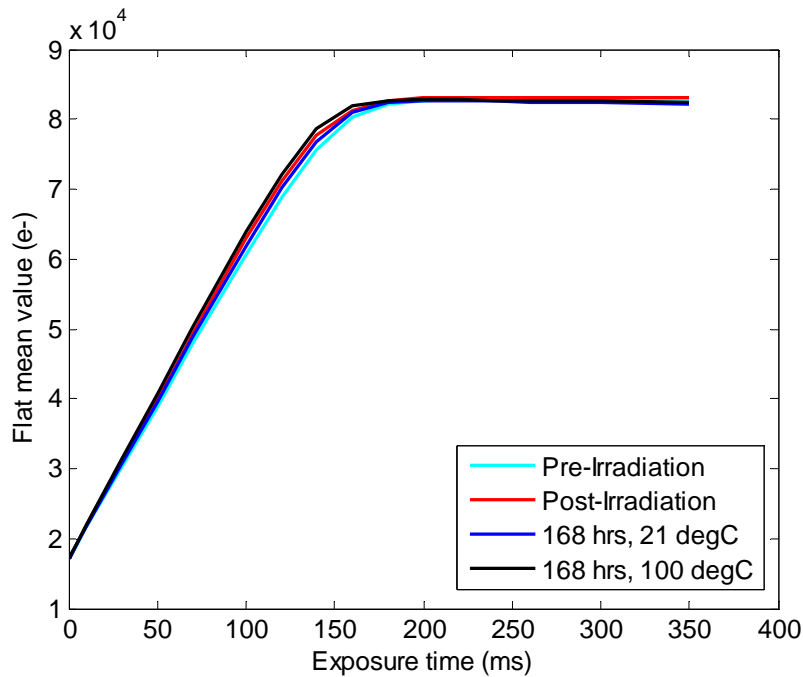


Figure 4-3 Mean flat level before and after irradiation/annealing.

4.4. PIXEL RESPONSE NON-UNIFORMITY

The results of the PRNU are very similar to the ones obtained for the DCNU. An increase appears after irradiation and then the annealing partially heals it.

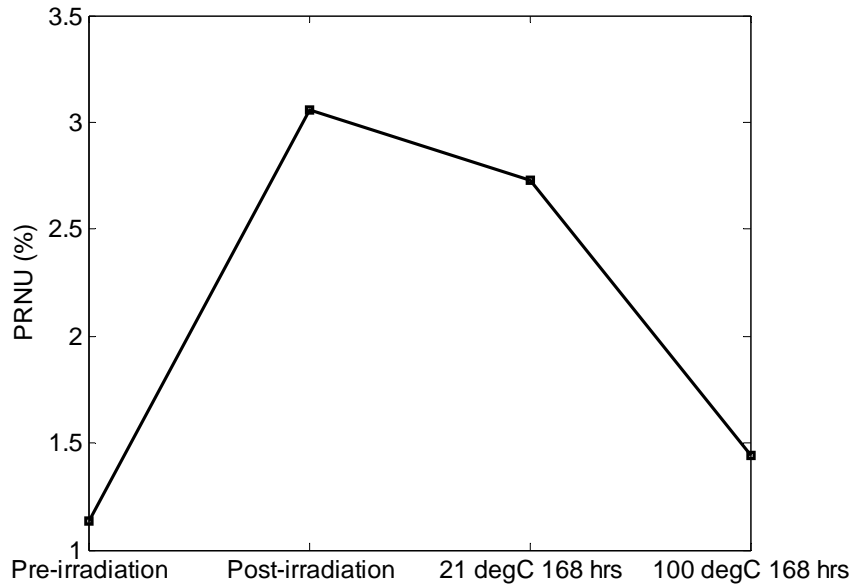


Figure 4-4 Pixel response non-uniformity: Measurements before and after irradiation/annealing

4.5. BAD PIXELS

The analysis of the bad pixels shows an increase after irradiation and a recovery after annealing, especially at high temperature (Figure 4-5). The value after the final annealing step is lower than the initial value.

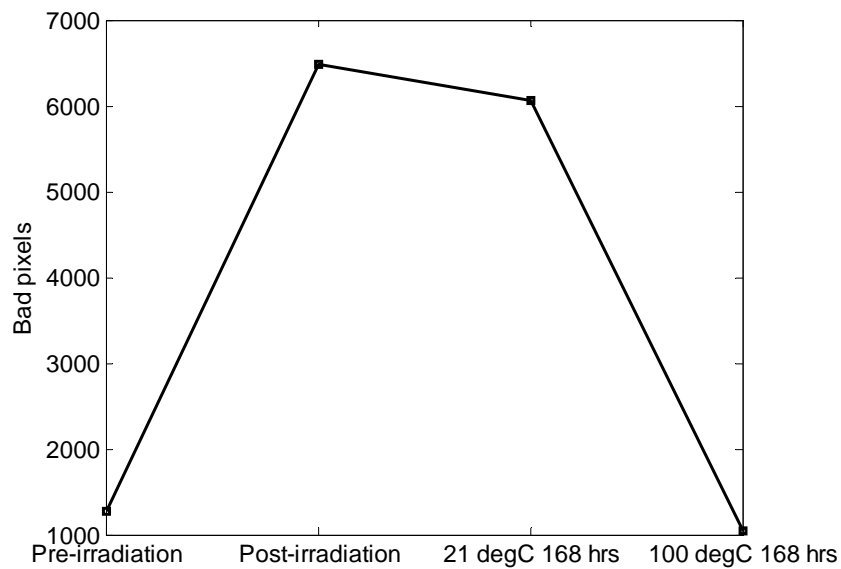


Figure 4-5 Bad pixels on the flat images at 100 ms of exposure time. The measurement criterion is above or below 6 times the standard deviation.



ISPHI CF-252 TEST RESULTS

5. SUMMARY AND CONCLUSIONS

The ISPHI sensor showed seven single event effects during the more than nine hours irradiation with the low flux Californium-252 source. Most of these events could be clearly classified as SEUs (even the affected register was identified for one of them), whereas others could not be definitely classified but can also be SEUs. In any case, all the events could be recovered either automatically by the TMR or after power cycling the sensor at the end of irradiation run.

All those events led to changes on the signal properties or the power consumption, but no single event functional interruptions (SEFI) were observed. In the same way, no single event latch-ups could be detected. Most of the event occurred while the source was placed above either the center of the sensor or the gold side.

As for the long-term induced effects, a short summary is given in Table 5-1.

Parameter	After irradiation	After annealing
Dark current	Increases about 500 e ⁻ /s.	Strongly increases after RT annealing, but decreases after HT. The initial value is not recovered.
DCNU	Increases about 1400 e ⁻ at 100 ms.	Decreases after annealing, though the initial value is not recuperated.
Temporal Dark Noise	No change.	No change.
Offset fixed pattern noise	No change.	No change.
Signal and saturation levels	Almost no change. The variations detected seem to be more related to measurement than to radiation effects.	Almost no change.
PRNU	Increases about 2%.	Decreases to almost the initial value.
Linearity and FW	No change.	No change.
Conversion gain	No change.	No change.
Power consumption	No change.	No change.

Table 5-1 Summary of Cf-252 effects

This pre-heavy ions test demonstrated the suitability of the PHI camera to be used for the real HI campaign, though it is desirable to carry out this campaign using the EQM model, which includes latch-up protection. Regarding the effects, it has been proved that even the Cf-252 is able to produce SEUs on the non-redundant sensor registers. However, no destructive events were observed.



DOCUMENT REFERENCES

5.1. NORMATIVE REFERENCES

REF	TITLE	DOC-REFERENCE	ISSUE	REVISION	REL-DATE
NR01	Experiment Interface Document: Part A	ESA/SOL-EST-RCD-0050	2	7	April 2011
NR02	Solar Orbiter environmental specification	ESA/TEC-EES-03-034/JS	3	0	June 2010

5.2. INFORMATIVE REFERENCES

REF	TITLE	DOC-REFERENCE	ISSUE	REVISION	REL-DATE
IR01	ISPHI Radiation Test Plan	SOL-PHI-MPS-TD3000-PL-3	1	1	2011-10-04
IR02	ISPHI: Image Sensor design report	CMOSIS-ISPFI-D1.1-001	1	-	December 2010
IR03	ISPHI Calibration and Characterization test plan	SOL-PHI-MPS-TD3000-PL-3	1(prel)	0	2011-10-27
IR04	ISPHI: Datasheet	CMOSIS-DS-ISPFI-0.3	0.3	-	May 2010
IR05	Radiation Engineering Methods for Space Applications (RADECS short course)	RADECS short course 2003	-	-	September 2003
IR06	EMVA standard 1288	EMVA1288-3.0	3	0	2010-11-29
IR07	ISPHI DD Test Results	SOL-PHI-MPS-TD3000-RP-4	1	0	2012-03-07
IR11	ISPHI: Test and characterization report	CMOSIS-ISPFI-D3.2-002	2	0	2012-02-03
IR12	ESTEC CASE website: https://escies.org/webdocument/showArticle?id=252&groupid=6	-	-	-	-
IR13	J. F. Ziegler, Handbook of Stopping Cross-Sections for Energetic Ions in All Elements, in The Stopping and Ranges of Ions in Matter	Vol. 5 (Ed. J.F. Ziegler). New York: Pergamo Press	-	-	1980



6. ACRONYMS

BBM	Bread Board Model
CASE	Californium Assessment for Single event Effects
Cf-252	Californium-252
CG	Conversion Gain
CMOS	Complementary Metal Oxide Semiconductor
DC	Dark Current
DCNU	Dark Current Non-Uniformity
DD	Displacement Damage
DN	Digital Number
DUT	Device Under Test
EGSE	Electrical Ground Support Equipment
EQM	Electrical-Qualification Model
FPN	Fixed Pattern Noise
FW	Full Well
HI	Heavy Ions
HK	Housekeeping
HT	High Temperature
IS	Image Sensor
ISPHI	Image Sensor for PHI
LET	Linear Energy Transfer
MPS	Max Planck institute for Solar system research
PRNU	Pixel Response Non-Uniformity
RT	Room Temperature
SEE	Single Event Effect
SEFI	Single Event Functional Interruption
SEL	Single Event Latch-up
SET	Single Event Transient
SEU	Single Event Upset
Si	Silicon
SO	Solar Orbiter
SO/PHI	Polarimetric and Helioseismic Imager for Solar Orbiter
TID	Total Ionizing Dose
TMR	Triple Module Redundancy